

SUBLIMATION KINETICS OF CO₂ ICE AND EVOLUTION OF THE MARTIAN POLAR CAPS. V. F. Chevrier¹, K. Bryson¹, L. A. Roe¹, D. G. Blackburn¹ and K. F. White², ¹Arkansas Center for Space and Planetary Science, University of Arkansas, Fayetteville, AR 72701, USA, ²Department of Physics & Astronomy, Ball State University, Muncie, IN 47306, USA <vchevrie@uark.edu>.

Introduction: The martian polar caps are in majority composed of CO₂ ice [1-3]. Early modeling of the polar caps suggested that they were in equilibrium with the ~6 mbar CO₂ atmosphere [2], and various observations have shown a cyclicity of growth and retreat, following martian seasons [4]. However, other studies show that CO₂ ice constitutes only a thin veneer on the surface of a probably much thicker ice layer [5]. This veneer is too small for the caps to be in equilibrium with the atmosphere [6,7]. This would also suggest that the polar caps are very young [8]. Therefore, there must be a much larger unidentified CO₂ reservoir in the martian subsurface, possibly adsorbed CO₂ in the regolith [9,10], to buffer the much larger atmosphere, or it means the total budget of CO₂ is present in the atmosphere, and that Mars has today much less CO₂ than other telluric planets.

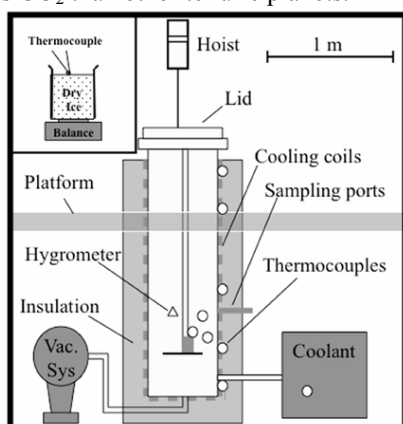


Figure 1. Scheme of the Andromeda martian environmental chamber used in the CO₂ ice sublimation experiments.

However, the majority of dynamic models of the polar caps are based on CO₂ ice sublimation, lacking laboratory confirmation. Most studies use thermal modeling [2] or geomorphic observations [7] to study sublimating CO₂, but the details of CO₂ sublimation in a CO₂ atmosphere remain unknown, and could have deep implications for the dynamics of the polar caps on the martian surface. We report here the experimentally measured sublimation rate of pure CO₂ ice under simulated martian conditions, and compare them to data from MGS MOLA, MOC and MRO HiRISE and CRISM.

Methods: Dry ice was packed into a beaker (Fig. 1) with a thermocouple above surface of the dry ice and, in later experiments, a second thermocouple placed inside the dry ice. Our planetary environmental chamber (Fig. 1) was evacuated to less than 0.09 mbar,

filled with dry gaseous CO₂ (g) to atmospheric pressure, and cooled to between 0 and -10°C. Once stable, the chamber was opened and the sample was placed on a top loading analytical balance inside the chamber. The platform supporting the balance and the sample was then lowered into the chamber. The chamber was then evacuated to 7 mbar. Experiments lasted ~1 hour and mass, pressure, and temperature were recorded every minute. Pressure and atmospheric temperature were maintained between 6.5 and 7.5 mbar and -11 to -1°C, respectively. Before and after each experiment the height and diameter of the dry ice was measured.

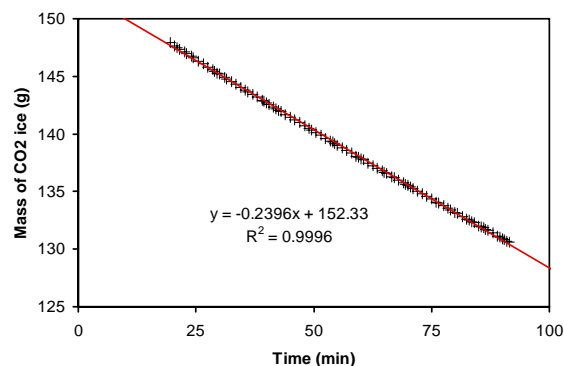


Figure 2. Mass of CO₂ ice as a function of time (sample #3 in Table 1).

Table 1. Sublimation rates E_S for the 10 samples studied in our chamber.

#	Texture	Mass loss (g min ⁻¹)	E_S (mm h ⁻¹)
1	Gravel	0.46	1.06
2	Solid block	0.24	1.01
3	Solid block	0.24	0.99
4	Powder	0.34	1.36
5	Powder	0.37	1.63
6	Powder	0.34	1.68
7	Loose powder	0.47	1.22
8	Loose powder	0.43	1.09
9	Packed powder	0.33	0.91
10	Packed powder	0.36	1.04

Results: The mass loss of CO₂ is very linear, with R^2 coefficients systematically above 0.99 (Fig. 2). The mass loss in g min⁻¹ is converted into sublimation rate E_S in mm h⁻¹ using the density and the surface area of the sample. Results are summarized in Table 1 and show remarkably constant values, validating the reproducibility of our experiments. The average value for CO₂ ice is 1.20 ± 0.27 mm h⁻¹. These results are

less than one order of magnitude higher than *in situ* measurements of polar caps retreat showing 0.13-0.19 mm h⁻¹ [4] and 0.36 mm h⁻¹ [6]. This suggests a common process for the sublimation mechanism on Mars and in our chamber.

It has been shown previously that surface temperature controls the sublimation rate of water ice [11,12]. We measured the temperature profiles inside the sample, a about 3 mm above the surface and 20 cm above the sample (Fig. 3). The temperature of the atmosphere remains very constant during the experiments, as well as the sample temperature at 148–153K, which corresponds to the equilibrium temperature of CO₂ at 7 mbar. This is exactly what is observed on the surface of Mars, where the polar caps are usually at the temperature 150K, thus in thermal equilibrium with the atmospheric pressure. The temperature a few mm above the surface is higher, 30 to 60K, as a result of the strong gradient between the surface and the atmosphere. The sudden increase in the sample temperature at t = 18 min (Fig. 3) results from the fact that the thermocouple reaches the surface when the ice is recessing due to sublimation. The temperature then converges towards the temperature a few mm above the surface.

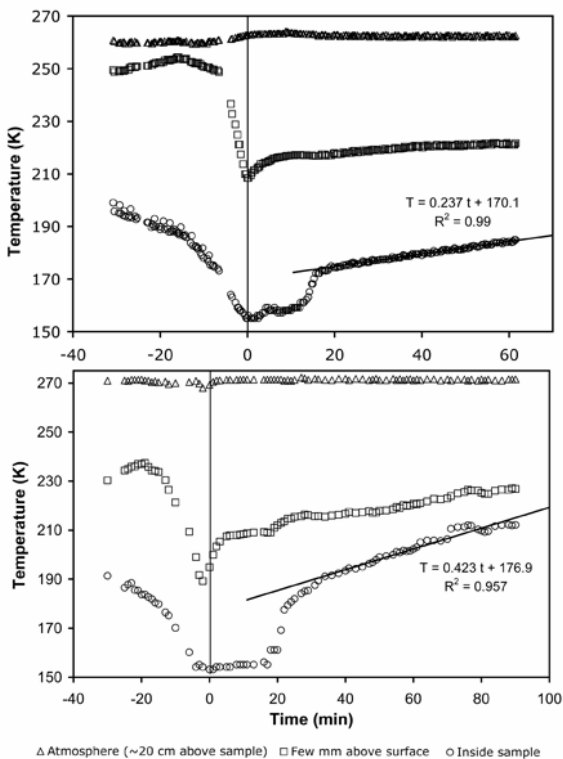


Figure 3. Thermal profiles of the atmosphere, 20 cm above the sample (triangles), 20 mm above the surface (squares) and initially inside the sample (circles), obtained during sublimation of CO₂ ice at 7 mbar.

Discussion:

Heat transfer process: The CO₂ sublimation process is governed by heat transfer between the chamber and the ice, and by diffusion of the sublimated molecules from the surface. There are three possible heat transfer processes: conduction from the ice surface into the ice interior, heat transfer from the warmer atmosphere to the cooler ice surface, and radiation from the chamber walls to the ice surface.

At the beginning of the experiment, the thermocouple below the ice surface reads ~150K, indicating that conduction has caused the ice to reach internal thermal equilibrium during the approximately 30 min pump-down. As a result, the surface and interior of the ice are at the same temperature, eliminating conduction into the ice as a heat transfer model. At this point, the ice surface has reached the solid - vapor equilibrium temperature associated with chamber pressure (7 mbar, 150K, Fig. 3). Therefore sublimation occurs because the atmosphere is too warm compared to the cold ice surface (263 to 273K against 150K, Fig. 3).

Thermal conduction in the CO₂ atmosphere is too low to be an efficient process in the chamber. Since the ice surface is considerably colder than the atmosphere, there are no buoyancy effects creating free convection, and there is no wind to create forced convection. Therefore, sublimation of CO₂ ice is controlled by radiation from the walls. We therefore use the following equation to describe CO₂ ice sublimation:

$$E_s = \frac{\Delta E_{rad}}{\rho_{ice} \Delta H_{298K,1bar}^{sub}} \quad (1)$$

where ΔE_{rad} is the energy absorbed by the surface (W m⁻²), ρ_{ice} is the CO₂ ice density (1562 kg m⁻³) and $\Delta H_{298K,1bar}^{sub}$ is the latent heat of sublimation (571.3 × 10³ J kg⁻¹). Our calculations show that radiative energy from the walls at 263K is about 220 W m⁻², giving a sublimation rate of 0.89 mm hr⁻¹, a value close to experimental results (1.2 mm hr⁻¹). Including the conduction from the atmosphere (~20 W m⁻²) raises the sublimation rate to 0.97 mm hr⁻¹.

Application to Mars:

Our experiments show that the behavior of CO₂ ice on Mars is largely dependent on the intensity of surface insolation. Figure 4A displays predicted sublimation rates at latitudes 86.5° N and S. By integrating the sublimation rates over a martian year, we predicted the changes in CO₂ thickness in the martian polar regions (Fig. 4B) and compared them to the MGS MOLA observations of surface altitude variations, averaged at constant latitude [4]. Both the model and MOLA altitude variations show a net transfer of 0.32 cm from the south to the north polar caps over a year (Fig. 4B). The agreement between our purely sublimational model and the MOLA data

indicates that all the CO₂ sublimated at one pole deposits at the other. Furthermore, due to the eccentricity of the martian orbit, the intensity of irradiance for the southern hemisphere summer is larger than for the northern hemisphere (Fig. 4A). This causes the southern hemisphere to exhibit higher sublimation rates than the northern hemisphere, resulting in a global transfer of CO₂ from the southern to the northern hemisphere.

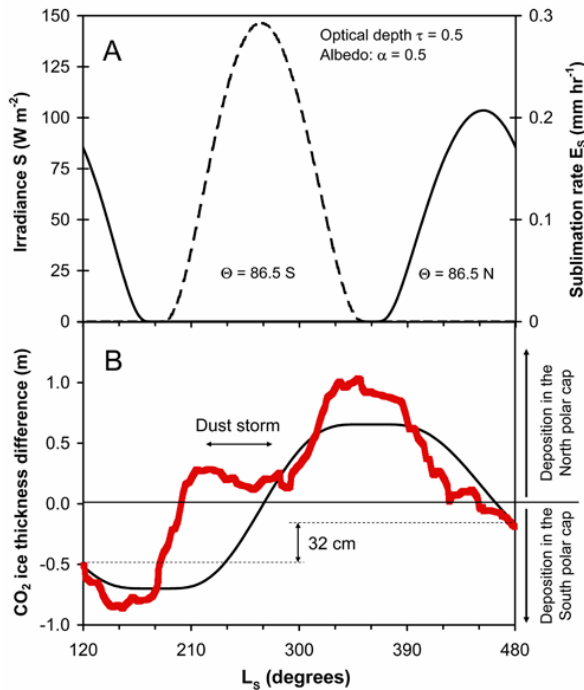


Figure 4. Sublimation model of the polar caps. A. Irradiance of the polar caps using a surface albedo of 0.5 [13,14] and an atmospheric opacity $\tau = 0.5$ with corresponding sublimation rates. B. Integration of these sublimation rates gives the thickness of sublimated CO₂ (black curve), compared to MGS MOLA data at latitude 86.5° (extracted from [4]). We represent both sets of data as the thickness difference between both caps: $\Delta h_{north} - \Delta h_{south}$, h being the thickness.

In order to better understand the precise dynamics of the polar caps, we focused on HiRISE high resolution pictures. Two geomorphologic features appear constantly on HiRISE images of the south polar cap. Smoother surfaces are observed at higher elevations than layers presenting an irregular surface (Fig. 5). CRISM observations of these features show that the top flat features are composed of CO₂ ice while the lower irregular layers are composed of water ice (Fig. 5). The water ice layer is visible only during the summer ($L_s = 332^\circ$), being covered by seasonal CO₂ during the winter. This demonstrates the presence of a seasonal cap of CO₂ on top of a perennial cap composed of CO₂ and water ice. Therefore, the thickness evolution of the polar caps is related to CO₂

dynamics, justifying our model based on experimentally verified CO₂ sublimation rates.

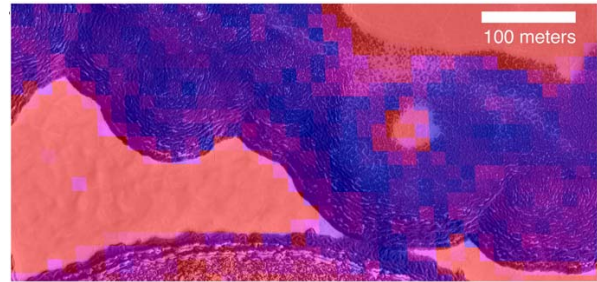


Figure 5. Summer observation at L_s 331.8, a subframe of HiRISE image PSP-005728-0935 with a superimposed CO₂/water ice indicator from infrared CRISM observation FRT000083f2_07. Red indicates CO₂ ice and blue water ice.

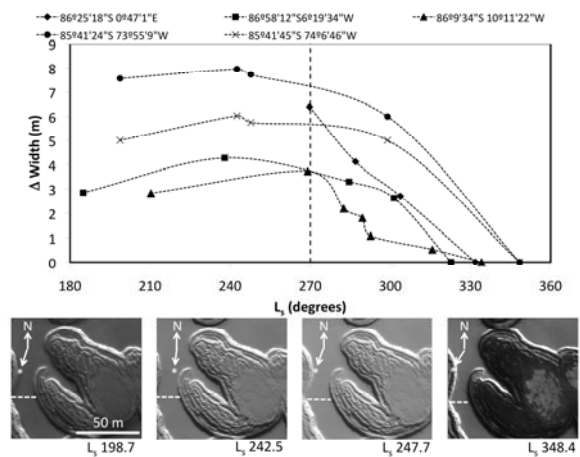


Figure 6. Analysis of MRO HiRISE images (subframes of HiRISE images at 85°41'S, 74°6'W, from left to right: PSP_002922_0945, PSP_003832_0945, PSP_003937_0945, PSP_006126_0945. Measured half delta width of the tops of CO₂ features at different south polar locations as a function of the solar longitude. The dashed line indicates where a feature width was measured. Arrows indicate direction toward the north (N) and the Sun (*), respectively.

Since there is good agreement between our model and MOLA results on a global scale, we want to verify its applicability at local scale. Therefore, we studied the evolution of the width of the south perennial CO₂ features (Fig. 6) at latitude $\sim 86^\circ S$ by comparing HiRISE images of the same region, obtained between $L_s \sim 180^\circ$ and $\sim 360^\circ$, i.e. during the south hemisphere summer (Fig. 6). We observe that the local CO₂ ice layer features undergo significant decrease in width by 3 ± 1 m (Fig. 6). Using a $\sim 30^\circ$ slope [7], this corresponds to a local elevation decrease of ~ 1.5 m during the summer, similar to longitudinally averaged MOLA observations of ~ 1.8 m and our model prediction of ~ 1.4 m (Fig. 1B). In addition, the sublimation of CO₂ starts at L_s 240° and ends around

L_S 330° (Fig. 6A), in agreement with our model (Fig. 4).

In the north polar cap, our model predicts sublimation between L_S 360° and 540° (Fig. 4A). This coincides with Viking Lander 2 pressure measurements, showing a pressure anomaly (as compared to purely thermally controlled) between L_S = 360° and 540° (Fig. 7).

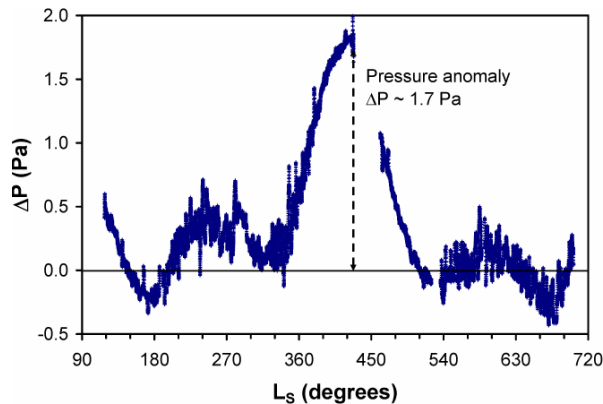


Figure 7. Deviation from of the surface pressure measured by Viking Lander 2 from the ideal gas law (control by the temperature). The large anomaly at L_S 360° to 540° corresponds exactly to the period of CO_2 sublimation in the north polar cap (Fig. 4).

All previous observations focused on annual or shorter timescales, and trends should also be observed in longer timescales. To determine the net perennial variation of the CO_2 caps, we compared MGS MOC images (acquired in 2001) and HiRISE images (acquired in 2007) of the southern polar cap, during the summer (L_S 285.6° and 289.5°) separated by three martian years. We observed a visible retreat of the CO_2 perennial cap (Fig. 8). Using the shadows produced by the CO_2 slab at low sun declination, we determined the average thickness of the CO_2 perennial cap to be 2.3 ± 0.4 m in MOC images and 1.03 ± 0.14 m in HiRISE images of the same features. The thickness difference gives an average sublimation rate of 0.43 ± 0.04 m y^{-1} , near the model prediction of 0.32 m y^{-1} .

Conclusions: Our study demonstrates that the dynamics of the polar caps are essentially controlled by the irradiance of the sun. We show that the southern CO_2 seasonal cap, about 1 to 1.5 m thick, covers presently a 1 meter thick CO_2 perennial cap, both on top of a layer of water ice. Furthermore, the eccentricity of the martian orbit produces higher sublimation rates in the south hemisphere than in the north, resulting in a global transfer of CO_2 from the south to the north pole. If the flux of CO_2 remains the same ($0.3 - 0.4$ m y^{-1}), then the perennial CO_2 cap should disappear in approximately 3 martian years. Due to the length of Mars' precession cycle, 93,000 martian years, it will take an extensive amount of time

for the equinoxes to change. Therefore, we predict that the CO_2 of the south polar cap will migrate entirely to the northern polar cap before such changes could occur, leaving a south pole entirely composed of water ice. If this water ice starts to sublimate, then higher humidity in the martian atmosphere should be expected. Alternatively, if progression of the south polar cap occurs in this timescale [15], then this suggests a short timescale climatic cycle.

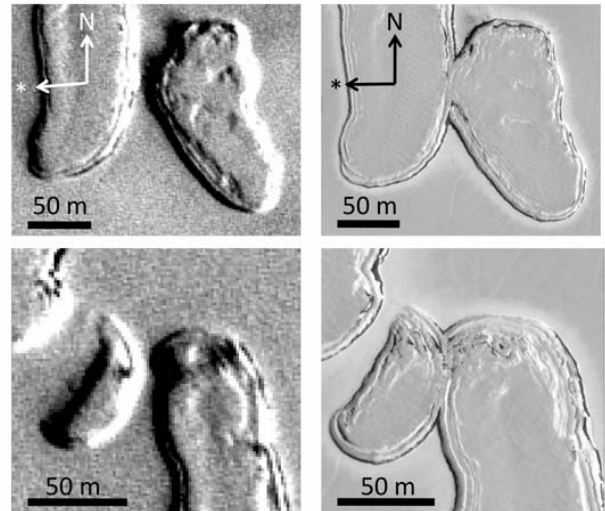


Figure 8. Comparison between MGS MOC (left) and MRO HiRISE (right) images of the same region, at approximately the same season, L_S 285.57° and 289.5°, respectively, indicating sublimation of CO_2 features over a 3 martian year time. The areas shown are subframes of (left) MOC image E11-00955 and (right) HiRISE image PSP-004792-0940. Arrows indicate direction toward the north (N) and the Sun (*), respectively.

References : [1] Langevin Y. et al. (2005) *Science* 307, 1581-1584. [2] Leighton R. B., B. C. Murray (1966) *Science* 153, 136-144. [3] Murray B. C., M. C. Malin (1973) *Science* 182, 437-443. [4] Smith D. E. et al. (2001) *Science* 294, 2141-2146. [5] Bibring J. P. et al. (2004) *Nature* 428, 627-630. [6] Malin M. C. et al. (2001) *Science* 294, 2146-2148. [7] Byrne S., A. P. Ingersoll (2003) *Science* 299, 1051-1053. [8] Fishbaugh K. E., J. W. Head III (2001) *Icarus* 154, 145-161. [9] Fanale F. P. et al. (1982) *J. Geophys. Res.* 87, 10215-10225. [10] Fanale F. P., W. A. Cannon (1971) *Nature* 230, 502-504. [11] Chevrier V. et al. (2007) *Geophys. Res. Lett.* 34. [12] Ingersoll A. P. (1970) *Science* 168, 972-973. [13] Paige D. A. et al. (1994) *J. Geophys. Res.* 99, 25959-25991. [14] Paige D. A., K. D. Keegan (1994) *J. Geophys. Res.* 99, 25993-26013. [15] Piqueux S., P. R. Christensen (2008) *J. Geophys. Res.* 113.